

Tribology of Nanopositioning

Characterization of precision linear bearings on nanometre scale

Dipl.-Ing. **Mikhail Kosinskiy**, Dr.-Ing. **Yonghe Liu**^{*}, Dr. **S.I.-U. Ahmed**,
Prof. Dr.-Ing. **Matthias Scherge**, Prof. Dr.rer.nat. **Juergen A. Schaefer**

Kurzfassung

Die systematische Untersuchung von der Bewegung und der Reibung einer Linearführung mit rollenden Elementen, welche zur Nanopositionierung genutzt wird, zeigt einen deutlichen Unterschied zwischen statischer Reibung und Rollreibung. Die Auswirkungen der Betriebsparametern auf das Reibverhalten und seine mögliche Verwendung in der Nanopositionierung und Nanomessung wurden diskutiert.

Abstract

A systematic characterization of the motion and friction of a linear bearing with rolling elements used for nanopositioning reveals an explicit distinction of static and rolling friction. The effects of operating parameters on the frictional behaviour and its possible utilization in the nanopositioning and nanomeasuring are discussed.

1. Introduction

Most wide-scanning-range nanopositioning and nanomeasuring (NPM) systems are realized through moving a positioning stage guided by bearings with friction. The presence of friction limits to a large extent the positioning and tracking performance of the NPM system, particularly when direct drivers such as voice coils are employed. The frictional behaviour of the bearings including the static friction and dynamic friction therefore needs to be thoroughly characterized under operating conditions that mimic that of the NPM system before a robust control strategy can be implemented.

Considerable efforts have been devoted into the construction of reliable models to describe friction. Most of the models strive to adequately recover phenomena such as static and dynamic friction, its load and velocity dependence and stick-slip [1]. A comparison of the measurements and model calculations, including the elastoplastic model and LuGre model indicates, however, that none of the models can describe the motion on nanometer scale

^{*} Corresponding author: Tel: +49 3677 695074; Fax: +49 3677 693205, e-mail: Yonghe.Liu@TU-Ilmenau.de

satisfactorily [1]. As a result, the accumulation of experimental data on the frictional behaviour of selected bearings and materials used for NPM system is important for motion control.

Linear bearings with rolling elements have been widely employed in NPM technology due to their extremely low friction coefficient and very smooth motion. In an earlier study, we characterized the pre-rolling behaviour of a linear bearing by a microtribometer. In that study we found that the pre-rolling of a linear bearing is composed of an initial linear part, the length of which is under the influence of lubrication and running conditions, and several nonlinear transitions before the onset of rolling [2]. This result indicates that the pre-rolling of the linear bearings might be employed in motion control in a very small scanning-range due to the linear motion. In this study, we characterize the general motion and friction behaviour of the linear bearings as a function of driving stroke and running velocity.

2. Experimentals

A linear bearing denominated as Z6 (Hirt GmbH) was tested. It is composed of a shaft (100Cr6 steel), a bush (stainless steel X46Cr13 hardened to HRC 57), a cage (brass) and a number of balls (tool steel X10CrMo17 hardened to HRC 61) of 0.6 mm in diameter. The dimension of each component and the mounting of the bearing are represented in the schematic diagram in Fig. 1. All the tests were performed in ambient environments with a relative humidity (r.H.) of 40% and temperature of 296 K approximately. The specimens were cleaned in an ultrasonic bath in acetone and methanol for five minutes each before conducting each of the tests.

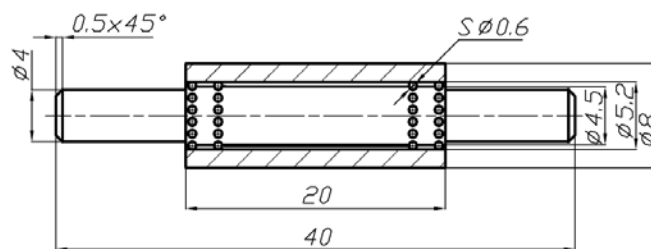


Fig. 1: Schematic diagram for the Z6 bearing tested in this work.

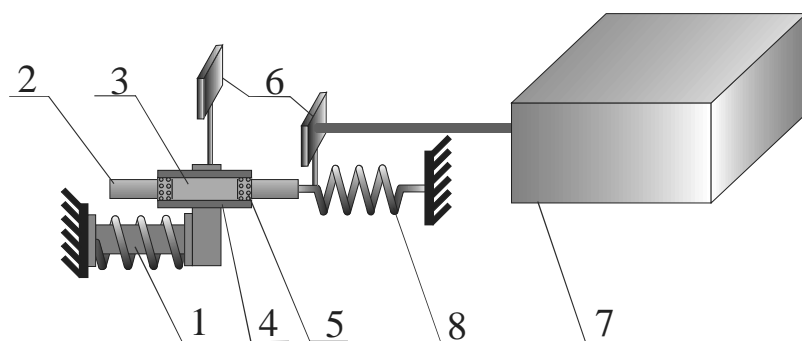


Fig. 2: The setup developed for direct measurements of the friction for linear bearings.
1 Piezo drive, 2 shaft, 3 cage, 4 bush, 5 balls, 6 mirror, 7 interferometer, and 8 spring.

We have developed a setup to measure the motion and the friction from bearings, as illustrated in Fig. 2. A piezo drive (1) is employed to provide frictionless driving action. The bush (4) of the linear bearing is fixed on the arm of the piezo and moves synchronously with it, while one end of the shaft (2) of the bearing is in contact with the force sensor, a double-leaf spring (8) with a spring constant of 8,543 N/m. Under this driving motion, sliding friction is produced at contacts between the balls (5) and the cage (3) and rolling friction was produced between the balls and bush and between the balls and the shaft. The friction force drives the shaft towards the force sensor. Mirrors were attached on the bush and the tip of the force sensor for measuring the driving motion and driven motion, respectively. The motion in terms of displacement was measured by a laser interferometer (7) (SIOS SP12). The friction force was obtained by measuring the displacement or deflection of the double-leaf spring at the driven side and multiplying it by the spring constant calibrated before hand. We can test the bearing with strokes in the range of 0.5~500 μm and with velocities in the range of 2~900 $\mu\text{m/s}$ by changing the voltage of Piezo amplifier (Piezosystem Jena, NV40), and the control signals from a function generator (TR-0458/B).

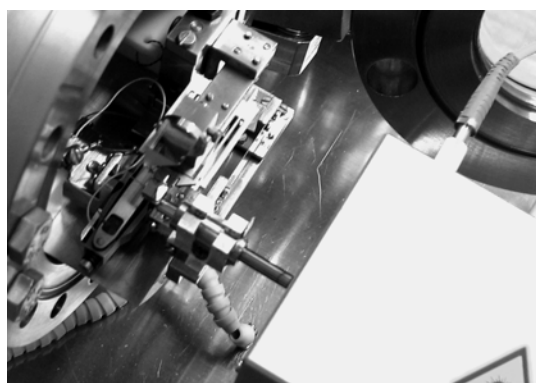


Fig. 3: The microtribometer built in an UHV chamber with the bearings mounted on the Piezo driver and the shaft of the bearing is in touch of the tip of the double-leaf-spring.

The whole setup can be placed into an ultra high vacuum (UHV) chamber, as shown in Fig. 3, with the exception of the laser interferometer, which was left outside of the chamber. This configuration is convenient for evaluating the friction of the bearings in vacuum and in various gas environments. This work concentrates on the testing in ambient conditions. The results obtained in vacuum will be reported in the future elsewhere.

3. Results

Fig.4 shows the displacement as a function of time measured at the driving side and driven side, respectively. The velocity was maintained at $\sim 2.3 \mu\text{m/s}$, while driving strokes were kept in Fig. 4 (a) to Fig. 4 (f) at 0.5, 3, 11, 32, 160 and 400 μm , respectively. The driving cycle and driven cycle were not synchronized exactly because the measurements on the driving side and driven side were performed independently. However, this does not affect our study on the general motion behaviour of the linear bearing. As can be seen, the driven displacement increases linearly with the driving displacement, reaches the peak and returns zero point simultaneously when the driving strokes are less than 3 μm in Fig. 4(a) and Fig. 4 (b). This result is in agreement of our early findings that the displacement of linear bearings is linearly related with driving displacement when the driving strokes are small [2]. Further increase of the driving stroke to 11 μm , as shown in Fig. 4 (c), the motion at driven side loses its symmetry. At one side, the driven displacement keeps linear while it saturates at the other side with the change of driving displacement. This saturation in displacement is similar to the onset of plastic deformation of the metals. Therefore, the elastoplastic model of friction is to some extent justified even for the linear bearings with rolling elements employed in this study. We notice that the driven motion and driving motion is in phase when the driving stroke is less than 11 μm , despite the onset of the plastic behaviour of the motion. Once the driving stroke

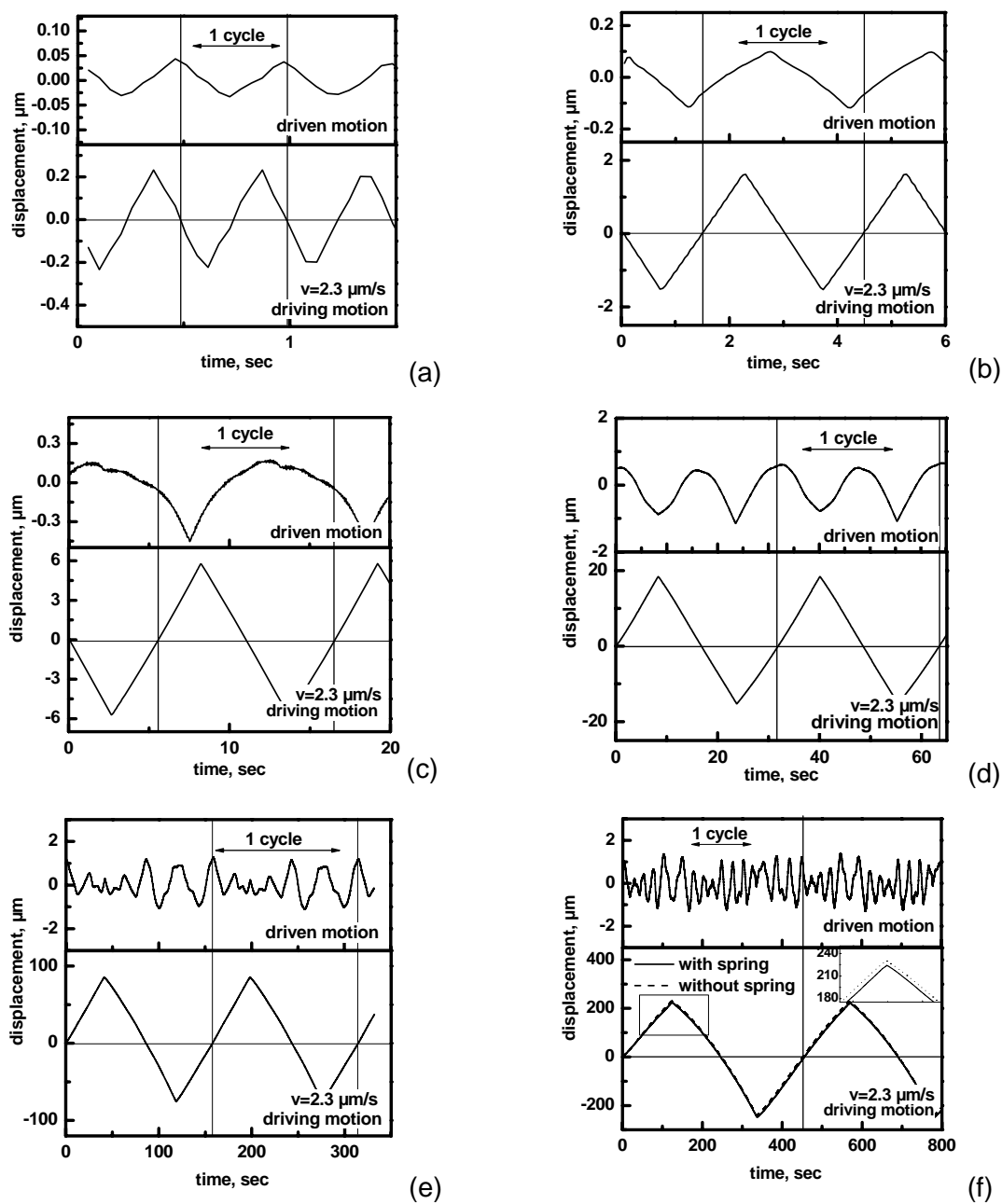


Fig. 4: The displacement as a function of time measured at the driving side and driven side, respectively. The velocity was maintained at $\sim 2.3 \mu\text{m/s}$, while driving strokes were kept at 0.5, 3, 11, 32, 160 and 400 μm for Figs (a)-(f), respectively. The driving cycle and driven cycle were not synchronized exactly because the measurements on the driving motion and driven motion were performed.

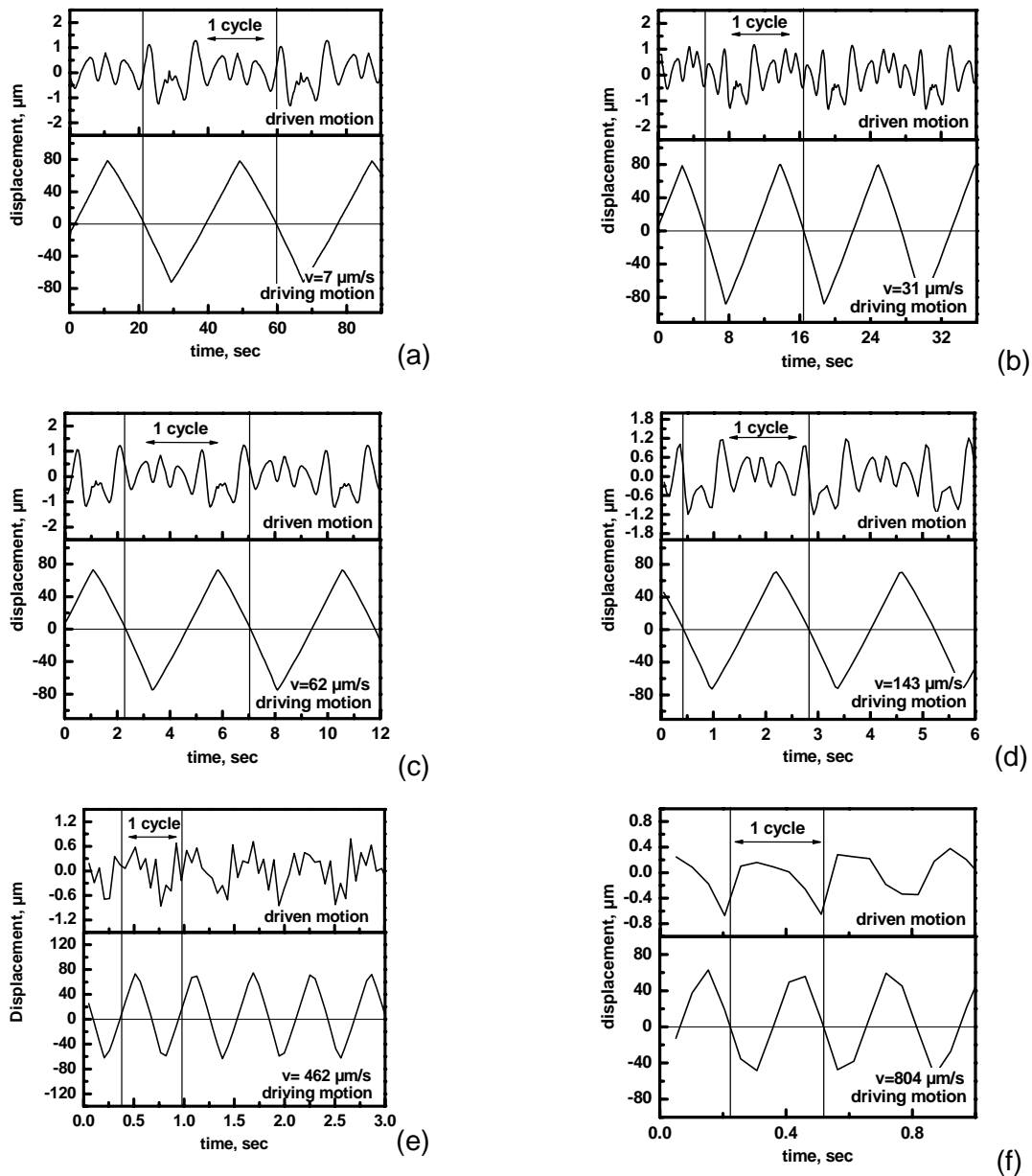


Fig. 5: The influence of the velocity on the motion of the bearing. The driving stroke maintained at $\sim 160 \mu\text{m}$, while velocity was kept at 7, 31, 62, 143, 462 and $804 \mu\text{m/s}$ for Figs (a)-(f), respectively. An additional figure at an extreme low velocity $2.3 \mu\text{m/s}$ is found in Fig. 4 (e).

increases to more than $32\text{ }\mu\text{m}$, the driven motion is out of phase of the driving motion as shown in Fig. 4 (d). In one driving cycle, there are two driven cycles, which are obviously different, with one cycle similar to that in Fig. 4 (c) and an additional one with both sides are saturated in displacement. Further increase of the driving strokes results in more driven cycles in one driving cycle as shown in Fig. 4 (e) and Fig. 4 (f). An estimation of the driving displacement needed for a driven cycle indicate that it is $\sim 32\text{ }\mu\text{m}$. This value is obviously related with the high stiffness of the spring we employed. A softer spring might be able to increase the sensitivity; however, it can also significantly decrease the natural frequency of the system, which complicates the analysis of the data. A Comparison of the driving motion with and without the introduction of the spring, as shown in Fig. 4 (f) indicates that the spring force sensor introduces a negligible influence on the system. More driven cycles, or multi peaks in one driving cycle are also termed as stick-slip, which defines the apparent smooth motion of the driven body into a stick phase moving together with the driver and a slip phase in which an addition slippery motion occurs.

Fig. 5 shows the influence of velocity on the motion of the bearings. The driving stroke is maintained at $\sim 160\text{ }\mu\text{m}$, while velocity was kept at 7, 31, 62, 143, 462 and $804\text{ }\mu\text{m/s}$ for Figs 5(a)-5(f), respectively. An additional figure at $2.3\text{ }\mu\text{m/s}$ is found in Fig. 4(e). Except at the extreme low velocity and at high velocity, the driven signal in one driving cycles maintain the same pattern with the change of velocity in a relative wide range from $7\text{ }\mu\text{m/s}$ to $143\text{ }\mu\text{m/s}$, as shown in Figs 5 (a) to (d). There are about 6 driven cycles in one driving cycle, which results in $\sim 53\text{ }\mu\text{m}$ driving displacement to achieve one driven cycle. This value is obviously longer than that needed at $2.3\text{ }\mu\text{m/s}$, $\sim 32\text{ }\mu\text{m}$. When the velocity is increased to $462\text{ }\mu\text{m/s}$, no regular period of the driven signal is observed. Instead, it turns smother except at the reversals where large peaks are observed. This trend is more obvious with further increase of the velocity to $804\text{ }\mu\text{m/s}$.

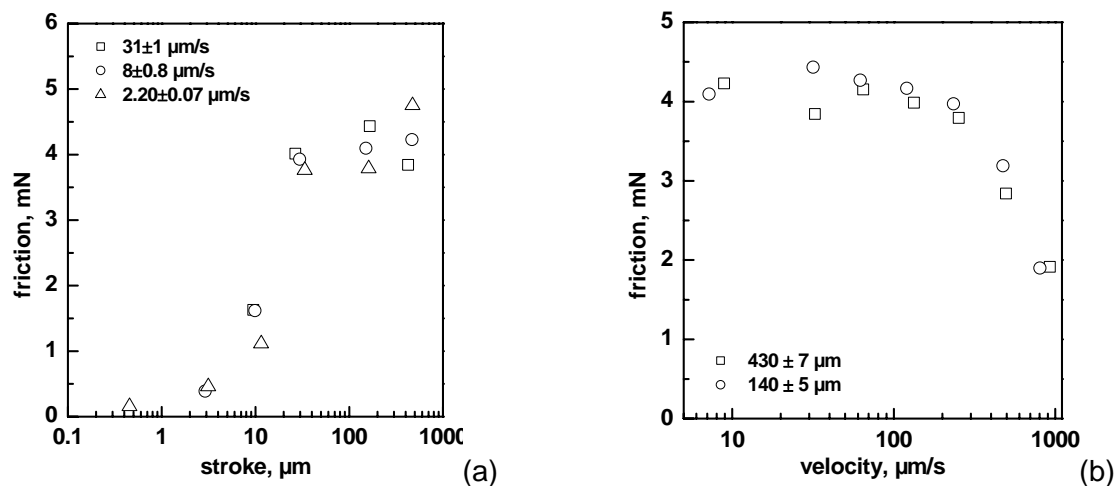


Fig. 6: Friction force as a function of driving stroke (a) and velocity (b) represented in a logarithm scale. Notice the linear relationship between the friction force and the driving stroke for driving strokes less than 30 μm in linear scale in (a), which defines an increase of static friction with driving stroke at a slope of 0.13 mN/ μm . When the driving stroke is more than 30 μm , rolling motion occurs, and the friction force maintains constant at $\sim 4 \mu\text{N}$ (a), and in a vast range of velocity from $\sim 10 \mu\text{m/s}$ to $\sim 200 \mu\text{m/s}$ (b).

In order to evaluate the motion at the driven side quantitatively, we examined the friction as a function of driving stroke and driving velocity, and show in Figs. 6(a) and 6(b), respectively. For the sake of the reading, the stroke and velocity are presented in the logarithm scale. The three curves in Fig. 6(a) were obtained at different velocities, which show the same trend. The friction is linearly related with the driving stroke (displacement) for the strokes less than 30 μm when observed on a linear scale. This is a typical characteristic of static friction. As a result, we can assume that the friction in this range is mainly in form of static friction, and it increases linearly with driving displacement. By linear fitting we found a slope $\sim 0.13 \text{ mN}/\mu\text{m}$ for the curve tested at $8 \mu\text{m/s}$. When the driving stroke is more than 30 μm , the friction force turns to be saturated at $\sim 4 \text{ mN}$. With such driving strokes, rolling motion occurs as evidenced by the multi peaks in the driven signal. The friction is then considered as the rolling friction, and it is nearly constant at 4 mN. The curves in Fig. 6(b) were obtained at strokes of 140 μm and 430 μm , respectively, which fall in the driving stroke range for rolling motion. In a velocity range $\sim 10 \mu\text{m/s}$ to 200 $\mu\text{m/s}$, the friction force maintains constant at $\sim 4 \text{ mN}$. When the velocity is extremely high, $> 400 \mu\text{m/s}$, we observed a reduced friction force. The velocity weakening of friction at high velocity is related with the elimination of stick-slip phenomena as shown in Figs 5(e) and 5(f).

4. Discussion

Various methods have been attempted in testing the linear bearings used for NPM system, for example, to measure the driving current for the direct-current motors and converting it into friction [1], to measure the force exerted at the spindle drivers [3]. However, these methods are normally coupled with the properties of drivers, which make the interpretation of the results more difficult. The setup used in this study as shown in Fig. 2 is considered a great advantage for testing precision bearings since it measures the motion on the driving as well as driven side simultaneously. In addition, the displacement from the driven side can be converted into friction force by multiplying the spring constant, which makes it possible to study the friction of the bearing at various driving strokes and velocities controlled by the Piezo driver.

An explicit distinction between static friction and rolling friction with the increase of driving stroke is established in Fig.4 and Fig. 6(a). When the driving stroke is less than 30 μm , the driven motion is in the same phase of the driving motion and is linearly related with the driving displacement in a driven range of more than 0.5 μm . This provides a great advantage in using such linear bearings in nanomeasuring. Jaeger [4] compared the nanomeasuring achieved by moving the stage through linear bearings and/or by moving the cantilever driven by Piezo, and found that an improved repeatability was obtained when the measurement was performed by moving the positioning stage transported by linear bearings. Our results demonstrate clearly that the linear bearings with ball elements can be employed in the NPM system by utilizing the linear motion in the limit of static friction. When the driving stroke is more than 30 μm , the typical case for wide-range nanopositioning, rolling motion occurs. In a velocity range between 10-200 $\mu\text{m/s}$, the rolling friction is nearly constant. As a result, a constant coefficient of friction can be employed in the motion control. If the velocity is increased further to $\sim\text{mm/s}$ for wider scanning range e.g. $>200\text{ mm}$, we must consider the velocity weakening of friction due to the elimination of the stick-slip. In this case, a low coefficient of rolling friction can be employed, for example following the empirical logarithm law [5]. However, the motion at reversals must be considered separately since peaks are usually observed as shown in Figs. 5(e) and 5(f).

The primary aim of this work is to characterize the motion and friction behaviour of the linear bearings used for NPM system. Future work currently underway is the effects from environmental factors, particularly vacuum, and the influence of tribological coatings. This is obviously valuable for the future development of the NPM system. To gain more insights, however, more controlled experiments are needed in order to examine the role of the geometry of bearings, surface roughness and materials.

5. Conclusions

A systematic characterization of a selected linear bearing with ball elements used in NPM system has been performed by a newly developed setup, which can measure the displacement at the driving and driven sides simultaneously at various operating parameters. Since the driven displacement can be converted into friction force, the motion and friction behaviour of the bearing can be evaluated. The main findings are:

- (1) An explicit distinction of static friction and rolling friction is observed with the increase of driving stroke.
- (2) In the limit of static friction, the driven motion is in the same phase of the driving motion, and is linearly related with the driving displacement.
- (3) Rolling motion occurs when the driving stroke is more than 30 μm , and the rolling friction force maintains constant in the velocity range of 10-200 $\mu\text{m/s}$. Further increase of the velocity results in the velocity weakening of rolling friction.

Acknowledgement

This research was supported by the German Science Foundation Deutsche Forschungsgemeinschaft (DFG) under grant number SFB 622. The authors acknowledge T. Haensel for technical support.

References

- [1] Y. Liu, J. A. Schaefer, G. Jaeger, *Technisches Messen*, 73 (2006) 500.
- [2] Y. Liu, W. Hild, M. Kitsche, S. Doering, G. Hungenbach, M. Scherge, J.A. Schaefer, in G. Akhras (ed.), *Proceedings of 7th Cansmart meeting-International Workshop on Smart Materials and Structures*, Montreal, 2004, p105.
- [3] Y. Liu: *Untersuchungen zu Gleitführungen für Nanopositionieranwendungen*. Dipl.-Arb., Technische Universität Ilmenau 2005, p60.
- [4] Jaeger, *Proceedings TEDA conference on Scanning Probe Microscopy, Sensors and Nanostructures*, Beijing, 2004, p23.
- [5] C. H. Scholz, *Earthquakes and friction laws*, *Nature* 391 (1998) 37.